PHYSICAL REVIEW A **89**, 040301(R) (2014)

Raman quantum memory based on an ensemble of nitrogen-vacancy centers coupled to a microcavity

Khabat Heshami,[1] Charles Santori,[2] Behzad Khanaliloo,[1] Chris Healey,[1] Victor M. Acosta,[2] Paul E. Barclay,[1,3] and Christoph Simon[1]

[1]*Institute for Quantum Science and Technology and Department of Physics and Astronomy, University of Calgary, Calgary, Alberta, Canada T2N 1N4*

[2]*Hewlett Packard Laboratories, 1501 Page Mill Rd., Palo Alto, California 94304, USA*

[3]*NRC National Institute for Nanotechnology, 11421 Saskatchewan Drive NW, Edmonton, Alberta, Canada T6G 2M9*

(Received 18 December 2013; published 7 April 2014)

We propose a scheme to realize optical quantum memories in an ensemble of nitrogen-vacancy centers in diamond that are coupled to a microcavity. The scheme is based on off-resonant Raman coupling, which allows one to circumvent optical inhomogeneous broadening and store optical photons in the electronic spin coherence. This approach promises a storage time of order 1 s and a time-bandwidth product of order 10^7. We include all possible optical transitions in a nine-level configuration, numerically evaluate the efficiencies, and discuss the requirements for achieving high efficiency and fidelity.

DOI: 10.1103/PhysRevA.89.040301 PACS number(s): 03.67.Lx, 42.50.Ex, 61.72.jn

Quantum memories for optical photons [1–3] are essential elements for photonic quantum information processing. Long-distance quantum communication based on quantum repeaters [4,5] requires optical quantum memories. They also can be used in conjunction with probabilistic photon pair sources for the realization of deterministic single-photon sources [6], which are necessary for linear optical quantum computation [7]. Negatively charged nitrogen-vacancy (NV^-) centers in diamond are attractive systems for implementing micron-scale optical quantum memories, which will be required for future integrated on-chip photonic quantum information processing architectures [8]. NV^- centers demonstrate strong coupling to optical photons, which can be further enhanced via optical microcavities [9]. Entanglement between an optical photon and the electronic spin of a single NV^- center [10], and between electronic spins of two distant NV^- centers [11] have recently been demonstrated. Ground-state electronic spin coherence times of 0.6 s have been shown using dynamical decoupling [12]. The electronic spin coherence in NV^- ensembles has been used for storage and retrieval of microwave photons (see [13]).

In this Rapid Communication we focus on storing quantum states of optical photons, which has remained challenging. In contrast to rare-earth ion doped crystals [14,15], NV^- centers exhibit a relatively short excited-state lifetime, which prevents long-lived storage based on optical coherences. Electromagnetically induced transparency (EIT), which is based on application of a resonant control beam in a Λ-level configuration, has been implemented [16,17]. This could be an approach to use the ground-state spin coherence to store optical photons. However, optical inhomogeneous broadening and interference due to closely spaced excited states make it difficult to achieve high EIT contrasts [17], and the resulting loss prevents quantum storage of optical photons.

In this Rapid Communication, we propose to use an off-resonant Raman coupling approach [18,19] that allows one to circumvent the excited-state inhomogeneous broadening (see Fig. 1). In our scheme, we consider an ensemble of NV^- centers coupled to an optical microcavity. The NV^- ensemble is initialized in a ground state and interacts with a cavity field and a control field pulse. For storage, the input field is coupled to the cavity and the control field pulse is simultaneously applied to the ensemble. This results in storing the optical photon and generating a collective spin excitation. For retrieval, one can apply a similar control field pulse to read out the spin excitation and generate a photon in the cavity's output. The NV^- ensemble is considered under a very high external static electric field and a low magnetic field in order to achieve the desired optical polarization selection rules.

We now describe the level structure of NV^- centers. Each NV^- center consists of six contributing electrons in the C_{3v} symmetry that is imposed by the diamond crystal lattice [20,21]. The electronic configuration consists of six excited states and one ground-state triplet. Neglecting hyperfine coupling with the nuclear spin, the ground eigenstates under external electric and magnetic fields can be shown to be

$$\begin{aligned} |0\rangle &= |S=1, m_s=0\rangle, \\ |+\rangle &= e^{i\phi_e/2}\cos\left(\frac{\theta}{2}\right)|1,1\rangle - e^{-i\phi_e/2}\sin\left(\frac{\theta}{2}\right)|1,-1\rangle, \\ |-\rangle &= e^{i\phi_e/2}\sin\left(\frac{\theta}{2}\right)|1,1\rangle + e^{-i\phi_e/2}\cos\left(\frac{\theta}{2}\right)|1,-1\rangle, \end{aligned} \quad (1)$$

where $\phi_e = \arctan(\frac{E_y^{gs}}{E_x^{gs}})$, $\theta = \arctan(\frac{E_\perp^{gs}}{B_z^{gs}})$, and $E_\perp^{gs} = \sqrt{E_x^{gs2} + E_y^{gs2}}$ (see [22]). $E_{x,y}^{gs}$ and B_z^{gs} are the ground-state energy shifts due to electric and magnetic fields according to the relevant dipole moments and g factors [23]. The energy splitting between $|\pm\rangle$ states is given by $2\sqrt{E_\perp^{gs2} + B_z^{gs2}}$. In the above description $|S=1, m_s=0,\pm1\rangle$ are the NV^- center's ground configuration states $\Phi^c_{A_2,1,\{0,\pm1\}}$, where $S=1$ shows the total spin for the NV^- center's ground-state triplet (see Table I in [20]). Likewise, one needs to consider the effect of external static electric and magnetic fields on the excited states. For this purpose, we derive spin-orbit and spin-spin interaction Hamiltonians in the configuration basis for the excited-state triplets (see the Supplemental Material [24]).

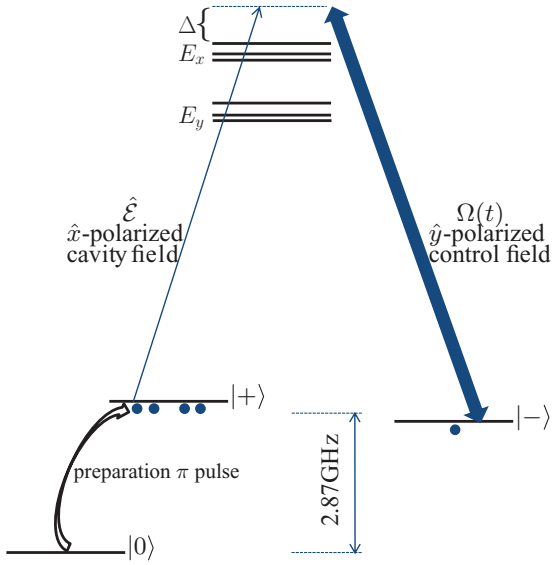

FIG. 1. (Color online) Raman quantum memory scheme. The figure shows the nine-level configuration of the electronic ground and excited states for a NV^- center. Initially, a microwave π pulse transfers the population from $|0\rangle$ to $|+\rangle$. A $\hat{x}$-polarized signal is coupled to a cavity to be stored. For storage, a collective spin excitation is generated through off-resonant coupling to an $\hat{x}$-polarized cavity field and a $\hat{y}$-polarized control field. For retrieval, a similar control field pulse is applied to read out the stored excitation. Δ is the cavity and control field detuning from the excited state.

Originally, an ensemble of oriented NV^- centers (see [25]) is prepared in the $\Phi^c_{A_2;S=1,m_s=0}$ ground state using off-resonant optical pumping [26]. As shown in Fig. 1, a preparation microwave π pulse prepares all NV^- centers in the $|+\rangle$ (with $m_I = 0$) ground state. An imperfect preparation may result in either exciting some of the NV^- centers to the $|-\rangle$ state or addressing multiple hyperfine levels corresponding to the $|+\rangle$ state. Since our regime of parameters will result in electronic spin splittings larger than the hyperfine splitting, the bandwidth of the preparation π pulse should be narrow compared with the hyperfine splitting of 2.2 MHz to avoid coupling to multiple hyperfine levels. At the same time, the microwave pulse bandwidth should at least be comparable with the spin inhomogeneous broadening of 200 kHz (see below).

It is crucial to determine polarization selection rules in order to study all active transitions in the light-NV^- interaction Hamiltonian. We consider ground eigenstates in Eq. (1) and excited states that are derived from Eqs. (S1) and (S2) in the Supplemental Material [24]. Taking into account that $\langle a_1|\hat{x}\cdot\vec{r}|e_x\rangle$ and $\langle a_1|\hat{y}\cdot\vec{r}|e_y\rangle$ are nonzero [21], where $a_{1,2}$ and $e_{x,y}$ denote single electron orbital basis given by linear combination of the dangling orbitals, we find all possible optical transitions for $\hat{x},\hat{y}$ polarized light from ground eigenstates to any of the excited states (see Table I and [24]). At a very low magnetic field, an external electric field mixes $\Phi^c_{A_2;1,\pm1}$ ground states to $|\pm\rangle$ states that are shown in Eqs. (1). In addition, the external electric field (in the x direction, where the z direction is defined by orientation of the NV^- centers and x is along one of the reflection planes) results in splitting of the excited states to the E_x and E_y branches [20,21,27]. As a result, one can couple

TABLE I. The following table shows coupling ratios $|g_x(j,k)/g_x(+,9)|$ for coupling to an $\hat{x}$-polarized light. The electric and magnetic field splittings are $E_x^{\rm es} = 120$ GHz, $B_z^{\rm es} = 10$ kHz, and $E_{y,z}^{\rm es} = B_{x,y}^{\rm es} = 0$.

	$k=4$	$k=5$	$k=6$	$k=7$	$k=8$	$k=9$
$j=1,\|0\rangle$	$<10^{-4}$	$<10^{-4}$	0.0006	1.0003	$<10^{-4}$	0.0585
$j=2,\|+\rangle$	$<10^{-4}$	$<10^{-4}$	0.0253	0.0585	0.0015	1
$j=3,\|-\rangle$	0.0050	0.0182	$<10^{-4}$	0.0001	1.0019	0.0015

transitions from $|\pm\rangle$ states to the excited states through linearly polarized photons. This helps with coupling NV^- centers to laterally confined cavities such as microring and photonic crystal cavities that generally lack polarization degeneracy in their modes. It has to be noted that there has been recent progress in coupling NV centers to Fabry-Perot-type cavities which can have polarization degeneracy [28].

Let us describe the dynamics of this system. First, free evolution of the system is given by $H_0 = \hbar\omega_c a^\dagger a + \sum_{i=1}^N \sum_{j=1..9} e^i_j \hat{\sigma}^i_{jj}$, where ω_c is the cavity's central frequency, a ($a^\dagger$) is the cavity photon's annihilation (creation) operator, and $\hat{\sigma}^i_{\mu\nu} = |\mu\rangle^i\langle\nu|$. The eigenenergies of the ith NV^- center e^i_j are given by ground- and excited-state Hamiltonians, where $j = 1\ldots3$ refers to $|0\rangle$, $|+\rangle$, and $|-\rangle$ ground states, respectively. $j = 4\ldots9$ denote the excited eigenstates, where $j=4$ and $j=9$ refer to the lowest and highest energy excited states. In the present scheme, NV^- centers interact with x-polarized cavity and y-polarized control fields. The interaction Hamiltonian is given by

$$H_{\rm int} = -\hbar\sum_{i=1}^{N}\sum_{j=1\ldots3}\sum_{k=4\ldots9}\hat{\mathcal{E}}G(j,k)\hat{\sigma}^i_{kj}e^{-i\omega_c t} + \Omega(j,k)\hat{\sigma}^i_{kj}e^{-i\omega_2 t} + \text{H.c.}, \quad (2)$$

where $\hat{\mathcal{E}} = ae^{i\omega_c t}$, $G(j,k) = g_x(j,k)d_{\rm zpl}\sqrt{\frac{\omega_c}{2\hbar\epsilon V}}$, and $\Omega(j,k) = d_{\rm zpl}g_y(j,k)\frac{E_2}{2\hbar}$. E_2 and ω_2 are amplitude and frequency of the control field, and $g_{x,y}(j,k) = \frac{\vec{\mu}_{jk}\cdot\hat{x},\hat{y}}{|\mu_{jk}|}$, where $\vec{\mu}_{jk} = \langle j|\vec{r}|k\rangle$. The transition dipole moment of the zero-phonon line (zpl) is given by $d_{\rm zpl} = \sqrt{\frac{3\pi^2\epsilon_0\hbar c^3\gamma_{\rm zpl}}{n_d\omega_0^3}}$, where n_d is diamond's refractive index and ω_0 is the transition frequency that is associated with $\lambda = 637$ nm. The above definition of $d_{\rm zpl}$ is based on $\gamma_{\rm zpl} = 0.035\gamma$, where γ is the radiative decay rate [23]. This takes into account that only few percent of the emission from the excited state is associated with the zero-phonon line. Note that the broad phonon sidebands do not affect the proposed process as they are a few nanometers detuned from the inhomogeneously broadened zero-phonon line.

One can rewrite the total Hamiltonian in terms of collective optical polarization operators $\hat{\sigma}_{(1,2)k} = \sum_{i=1}^N \hat{\sigma}^i_{(1,2)k}e^{i\omega_c t}$, $\hat{\sigma}_{3k} = \sum_{i=1}^N \hat{\sigma}^i_{3k}e^{i\omega_2 t}$, and $\hat{\sigma}_{\mu\mu} = \sum_{i=1}^N \hat{\sigma}^i_{\mu\mu}$, where N is the total number of NV^- centers, $k = 4\ldots9$ and $\mu = 1\ldots9$. Using the Heisenberg equation $\dot{\hat{\mathcal{O}}} = \frac{i}{\hbar}[H,\hat{\mathcal{O}}] + \frac{\partial\hat{\mathcal{O}}}{\partial t}$ we find the dynamics of the cavity field operator and the collective operators describing the spin and optical polarizations and

populations (see the Supplemental Material [24]). In our model, we include relevant decay and decoherence rates. Specifically, optical inhomogeneous broadening (γ_e), spin inhomogeneous broadening (γ_s), and excited-state radiative decay (γ) are included in the dynamics of the optical polarizations, spin polarization, and level populations. Nonlinear contributions in these dynamical equations for collective operators can be ignored if the number of NV^- centers is much larger than the number of input photons [29,30]. Due to linearity of the dynamics, one can solve the same dynamical equations to find solutions to the single excitation wave functions of the corresponding collective operators [29,31] (see below). For example, the single spin excitation wave function is given by the dynamics of $\hat{\sigma}_{23}$.

One can also derive the dynamics of the cavity field operator. Given that the cavity decay rate is the fastest rate in the system, we can use adiabatic elimination to simplify the cavity field dynamics [30]. This leads to

$$\hat{\mathcal{E}}(t) = \frac{1}{\kappa}\left\{\sqrt{2\kappa}\hat{\mathcal{E}}_{\rm in}(t) + i\sum_{j=1,2}\sum_{k=4\ldots9} G^*(j,k)\hat{\sigma}_{jk} + i\sum_{k=4\ldots9} G^*(3,k)\hat{\sigma}_{3k}e^{-i(\omega_2-\omega_c)t}\right\}, \quad (3)$$

where $\hat{\mathcal{E}}_{\rm in}(t)$ is the annihilation operator corresponding to the input signal. The cavity input-output equation $\hat{\mathcal{E}}_{\rm out}(t) = -\hat{\mathcal{E}}_{\rm in}(t) + \sqrt{2\kappa}\hat{\mathcal{E}}(t)$ in combination with the above considerations allows one to analyze the proposed memory scheme and study its performance (see [29,30] for similar treatments).

The total efficiency is found based on $\eta_{\rm tot} = \frac{\int|\mathcal{E}_{\rm out}(t)|^2dt}{\int|\mathcal{E}_{\rm in}(t)|^2dt}$, where $\mathcal{E}_{\rm in,out}(t) = \langle 0|\hat{\mathcal{E}}_{\rm in,out}(t)|1\rangle$ is the single-photon wave function. Here $|1\rangle$ is the single-photon input state. One can also find the storage efficiency by using $\eta_s = 1 - \frac{\int dt|\mathcal{E}^s_{\rm out}(t)|^2}{\int dt|\mathcal{E}_{\rm in}(t)|^2}$, where $\mathcal{E}^s_{\rm out}(t)$ is the field that is lost during storage. This is justified as there will be almost no population in the excited states during the storage process (up to 0.03% of the initial population in level $|+\rangle$ for parameters that are given below) and therefore the radiative decay does not introduce a significant loss channel.

We consider generated noise at the output that is due to nonzero coupling of the control field to $|+\rangle \rightarrow |k\rangle$ transitions, where $|k\rangle$ refers to any of the excited states. Note that contributions from the lower branch of the excited states are suppressed due to a significant splitting of 240 GHz (see below). We calculate the noise by finding the output field in the absence of input field, which gives rise to a nonzero probability of detecting a photon at the output. This results in reduction of the storage fidelity. Using total probabilities for reading out the signal and the noise we can estimate the conditional fidelity based on $1 - \frac{P_{\rm noise}}{P_{\rm sig}}$ (see [3]).

In Fig. 2, we show the results of our numerical solution to the differential equations for single collective excitation wave functions and Eq. (3) based on the assumption that all of the NV^- centers are initially in the $|+\rangle$ state. We show a Gaussian input signal intensity, $|\mathcal{E}_{\rm in}(t)|^2$, which has a pulse duration of $\tau = 40$ ns at $1/e$ of the maximum of the intensity. We find that this 40 ns input pulse is being stored with a storage efficiency of $\eta_s \approx 91\%$. For retrieval, the state of the stored

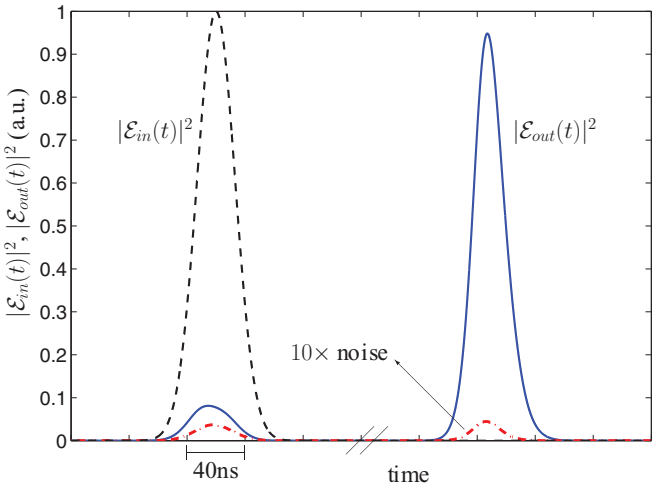

FIG. 2. (Color online) Simulation results of storage and retrieval of input pulse (black dashed line). The blue solid line presents the cavity output field. Simulation parameters: pulse bandwidth $\Delta\omega = 110$ MHz, excited-state inhomogeneous broadening $\gamma_e = 1$ GHz, and spin inhomogeneous broadening $\gamma_s = 200$ kHz. The detuning from the excited state, $\Delta = 0.8$ GHz (other parameters are provided in the main text). This results in 91% absorption efficiency and 81% total efficiency. The red dash-dotted line is associated with the noise intensity (multiplied by 10 for clarity), corresponding to 1% total noise probability. This gives 99% conditional fidelity (see text for more details).

spin excitation is used as the initial state of the dynamics with no input field present. Using the control field $\Omega(t)$ we can read the stored excitation out. For the above-mentioned parameters we calculate the total efficiency of $\eta_{\rm tot} = 81\%$. The total efficiency can be enhanced by increasing the control field strength. However, in the regime where $\frac{\Omega^2}{\Delta}\tau \approx 1$ the ac Stark shift affects the output field shape. The ac Stark shift can be compensated by a proper phase modulation on the control pulse [18,32]. This allows one to approach the ideal retrieval efficiency [29].

Our results in Fig. 2 depend on several physical parameters including the external electric and magnetic fields, which determine the transition dipole moments, in addition to the characteristics of the ensemble and the cavity. The performance of the quantum memory scheme also depends on the detuning Δ because of the coupling to neighboring excited states. The large number of parameters and complications due to the level structure make a systematic optimization very difficult. Below, we explain physical requirements for achieving the shown results.

Coupling of the control field to the $|+\rangle \rightarrow |k = 8\rangle$ transition (see Table I in [24]), may result in noise through off-resonant scattering of an $\hat{x}$-polarized photon via $|k = 8\rangle \rightarrow |-\rangle$ transition. In order to suppress this effect, Δ cannot be much larger than the energy splitting of these two excited states ($j = 8,9$), which is about 1.5 GHz. Here, we assume $\Delta = 0.8$ GHz (as shown in Fig. 1) and an optical inhomogeneous broadening of 1 GHz. In [33], authors present a sample with NV^- density of about 8000 NV/$(\mu$m$)^3$ that has an optical linewidth at FWHM of 10 GHz. Here, we require a minimum NV ensemble density of about 50 NV/$(\mu$m$)^3$ oriented NV^-

centers (this is based on the number of NV^- centers that are assumed for the simulations that are given below). One can employ spectral hole burning techniques [34] to reduce the optical inhomogeneous broadening down to the 1 GHz range.

For the numerical simulation in Fig. 2, we set $N = 100$, and for this size of an ensemble, only a relatively moderate cavity quality factor of $Q = 1100$ is required. The correspondingly modest density of NV^- centers is compatible with achieving low optical and spin inhomogeneous broadening. Our choice of the cavity quality factor is well justified as higher cavity quality factors have been achieved for a single NV^- center in a cavity (see [35,36]). The assumed cavity quality factor results in a cavity amplitude decay rate of $\kappa/2\pi = \frac{\omega_c}{2Q} = 210$ GHz, which is by far the fastest rate in the system and justifies the adiabatic elimination in the derivation of Eq. (3). The mode volume is $V = 100(\frac{\lambda}{n_d})^3$. A maximum Rabi frequency of $(\Omega_0/2\pi)^2 = 1\ (\mathrm{GHz})^2$ per 1 mW of control field power can be achieved for a beam waist of 8 μm. Here we considered maximum control field powers of 0.8 and 6.7 mW for read in and read out, respectively, and the control field pulse shape for storage and retrieval are set to be identical to the signal. The cavity must efficiently couple to $\hat{x}$-polarized light (polarization of input/output signals). The $\hat{y}$-polarized control field is simultaneously applied from a different direction. Having opposite polarizations for the signal and control fields is beneficial for the scheme as it prevents excessive noise that depends on the power of the control field and lowers the conditional fidelity.

The polarization selection rules are determined by the external electric and magnetic fields. Here, $E_y^{\mathrm{es}} = E_y^{\mathrm{gs}} = 0$ and $E_x^{\mathrm{es}} = 120$ GHz, with corresponding $E_x^{\mathrm{gs}} = 3.4$ MHz. A low magnetic field strength is assumed such that it causes $B_z^{\mathrm{es}} = 10$ kHz and $B_z^{\mathrm{gs}} = 9.9$ kHz splittings. These give the splitting of approximately 6.8 MHz between $|+\rangle$ and $|-\rangle$ ground states [see Eqs. (1)]. Energy shifts of 17 Hz/(V/cm) and 2.8 MHz/G are expected for nonaxial electric field and axial (parallel to the NV axis) magnetic field. The nonzero magnetic field is advantageous because of creating an imbalance between couplings to the two highest-energy (competing) excited states (see Tables I and II in the Supplemental Information [24]), which is in favor of storage with high efficiency and fidelity. According to these coupling coefficients, a magnetic field of about 3.5 mG and an electric field of 20 V/μm will be required to achieve the above-mentioned energy shifts. It has to be noted that the energy shift due the electric field can be applied by employing a properly oriented external strain.

Here we assumed the spin inhomogeneous broadening of 200 kHz (see [17]). This relatively narrow spin inhomogeneous broadening provides a storage time of 200 ns without a significant impact on the retrieval efficiency (reduced by a factor of 0.96) without application of any rephasing π pulse. Applying a dynamical decoupling pulse sequence, such as a series of rephasing π pulses, can extend the storage time by many orders of magnitude [30,37]. The longest spin coherence lifetime measured to date using dynamical decoupling is 0.6 s [12]. Thus, a time-bandwidth product up to 10^7 may be possible in our scheme.

In conclusion, we proposed a scheme based on off-resonant Raman coupling for storage of optical photons in an ensemble of NV^- centers that are coupled to a microcavity. High efficiencies are possible with realistic parameters, and using dynamical decoupling techniques, we expect that long storage times can simultaneously be achieved. The realization of an on-chip, efficient and long-storage-time optical quantum memory is therefore feasible owing to recent advances in NV technology. Recent results on coupling the ground-state electronic spin of NV ensembles to superconducting flux qubits in combination with the present proposal might provide a foundation for a hybrid architecture [38] that is capable of quantum communication and information processing using photons, NV^- centers, and superconducting circuits [39–41].

This work was supported by NSERC and AITF. K.H. would like to thank S. Raeisi and R. Ghobadi for useful discussions.

[1] A. I. Lvovsky, B. C. Sanders, and W. Tittel, Nat. Photonics **3**, 706 (2009).
[2] W. Tittel, M. Afzelius, T. Chaneliére, R. L. Cone, S. Kröll, S. A. Moiseev, and M. Sellars, Laser Photonics Rev. **4**, 244 (2010).
[3] C. Simon *et al.*, Eur. Phys. J. D **58**, 1 (2010).
[4] L.-M. Duan, M. Lukin, J. I. Cirac, and P. Zoller, Nature (London) **414**, 413 (2001).
[5] N. Sangouard, C. Simon, H. de Riedmatten, and N. Gisin, Rev. Mod. Phys. **83**, 33 (2011).
[6] S. Chen, Y.-A. Chen, T. Strassel, Z.-S. Yuan, B. Zhao, J. Schmiedmayer, and J.-W. Pan, Phys. Rev. Lett. **97**, 173004 (2006).
[7] E. Knill, R. Laflamme, and G. J. Milburn, Nature (London) **409**, 46 (2001).
[8] J. L. O'Brien, A. Furusawa, and J. Vuckovic, Nat. Photonics **3**, 687 (2009).
[9] M. Lončar and A. Faraon, MRS Bull. **38**, 144 (2013).
[10] E. Togan, Y. Chu, A. S. Trifonov, L. Jiang, J. Maze, L. Childress, M. V. G. Dutt, A. S. Sørensen, P. R. Hemmer, A. S. Zibrov, and M. D. Lukin, Nature (London) **466**, 730 (2010).
[11] H. Bernien, B. Hensen, W. Pfaff, G. Koolstra, M. S. Blok, L. Robledo, T. H. Taminiau, M. Markham, D. J. Twitchen, L. Childress, and R. Hanson, Nature (London) **497**, 86 (2013).
[12] N. Bar-Gill, L. M. Pham, A. Jarmola, D. Budker, and R. L. Walsworth, Nat. Commun. **4**, 1743 (2013).
[13] Y. Kubo, I. Diniz, A. Dewes, V. Jacques, A. Dréau, J.-F. Roch, A. Auffeves, D. Vion, D. Esteve, and P. Bertet, Phys. Rev. A **85**, 012333 (2012).
[14] M. P. Hedges, J. J. Longdell, Y. Li, and M. J. Sellars, Nature (London) **465**, 1052 (2010).
[15] E. Saglamyurek, N. Sinclair, J. Jin, J. A. Slater, D. Oblak, Félix Bussiéres, M. George, R. Ricken, W. Sohler, and W. Tittel, Nature (London) **469**, 512 (2011).

[16] P. R. Hemmer, A. V. Turukhin, M. S. Shahriar, and J. A. Musser, Opt. Lett. **26**, 361 (2001).
[17] V. M. Acosta, K. Jensen, C. Santori, D. Budker, and R. G. Beausoleil, Phys. Rev. Lett. **110**, 213605 (2013).
[18] K. F. Reim, J. Nunn, V. O. Lorenz, B. J. Sussman, K. C. Lee, N. K. Langford, D. Jaksch, and I. A. Walmsley, Nat. Photonics **4**, 218 (2010).
[19] J. Nunn, I. A. Walmsley, M. G. Raymer, K. Surmacz, F. C. Waldermann, Z. Wang, and D. Jaksch, Phys. Rev. A **75**, 011401(R) (2007).
[20] M. W. Doherty, N. B. Manson, P. Delaney, and L. C. L. Hollenberg, New J. Phys. **13**, 025019 (2011).
[21] J. R. Maze, A. Gali, E. Togan, Y. Chu, A. Trifonov, E. Kaxiras, and M. D. Lukin, New J. Phys. **13**, 025025 (2011).
[22] M. W. Doherty, F. Dolde, H. Fedder, F. Jelezko, J. Wrachtrup, N. B. Manson, and L. C. L. Hollenberg, Phys. Rev. B **85**, 205203 (2012).
[23] M. W. Doherty, N. B. Manson, P. Delaney, F. Jelezko, J. Wrachtrup, and L. C. L. Hollenberg, Phys. Rep. **528**, 1 (2013).
[24] See Supplemental Material at http://link.aps.org/supplemental/10.1103/PhysRevA.89.040301 for NV^- center's excited state Hamiltonian, optical couplings and dynamical equations for optical and spin polarizations.
[25] J. Michl, T. Teraji, S. Zaiser, I. Jakobi, G. Waldherr, F. Dolde, P. Neumann, M. W. Doherty, N. B. Manson, J. Isoya, and J. Wrachtrup, Appl. Phys. Lett. **104**, 102407 (2014).
[26] J. Harrison, M. J. Sellars, and N. B. Manson, J. Lumin. **107**, 245 (2004).
[27] V. M. Acosta, C. Santori, A. Faraon, Z. Huang, K.-M. C. Fu, A. Stacey, D. A. Simpson, K. Ganesan, S. Tomljenovic-Hanic, A. D. Greentree, S. Prawer, and R. G. Beausoleil, Phys. Rev. Lett. **108**, 206401 (2012).
[28] R. Albrecht, A. Bommer, C. Deutsch, J. Reichel, and C. Becher, Phys. Rev. Lett. **110**, 243602 (2013).
[29] A. V. Gorshkov, A. André, M. D. Lukin, and A. S. Sørensen, Phys. Rev. A **76**, 033804 (2007).
[30] K. Heshami, A. Green, Y. Han, A. Rispe, E. Saglamyurek, N. Sinclair, W. Tittel, and C. Simon, Phys. Rev. A **86**, 013813 (2012).
[31] K. Hammerer, A. S. Sørensen, and E. S. Polzik, Rev. Mod. Phys. **82**, 1041 (2010).
[32] K. Surmacz, J. Nunn, K. Reim, K. C. Lee, V. O. Lorenz, B. Sussman, I. A. Walmsley, and D. Jaksch, Phys. Rev. A **78**, 033806 (2008).
[33] C. Santori, D. Fattal, S. M. Spillane, M. Fiorentino, R. G. Beausoleil, A. D. Greentree, P. Olivero, M. Draganski, J. R. Rabeau, P. Reichart, B. C. Gibson, S. Rubanov, D. N. Jamieson, and S. Prawer, Opt. Express **14**, 7986 (2006).
[34] N. R. S. Reddy, N. B. Manson, and E. R. Krausz, J. Lumin. **38**, 46 (1987).
[35] A. Faraon, P. E. Barclay, C. Santori, K.-M. C. Fu, and R. G. Beausoleil, Nat. Photonics **5**, 301 (2011).
[36] A. Faraon, C. Santori, Z. Huang, K.-M. C. Fu, V. M. Acosta, D. Fattal, and R. G. Beausoleil, New J. Phys. **15**, 025010 (2013).
[37] J. J. Longdell, E. Fraval, M. J. Sellars, and N. B. Manson, Phys. Rev. Lett. **95**, 063601 (2005).
[38] M. Wallquist, K. Hammerer, P. Rabl, M. Lukin, and P. Zoller, Phys. Scr. **2009**, 014001 (2009).
[39] Y. Kubo, C. Grezes, A. Dewes, T. Umeda, J. Isoya, H. Sumiya, N. Morishita, H. Abe, S. Onoda, T. Ohshima, V. Jacques, A. Dréau, J.-F. Roch, I. Diniz, A. Auffeves, D. Vion, D. Esteve, and P. Bertet, Phys. Rev. Lett. **107**, 220501 (2011).
[40] X. Zhu, S. Saito, A. Kemp, K. Kakuyanagi, S.-I. Karimoto, H. Nakano, W. J. Munro, Y. Tokura, M. S. Everitt, K. Nemoto, M. Kasu, N. Mizuochi, and K. Semba, Nature (London) **478**, 221 (2011).
[41] X.-Y. Lü, Z.-L. Xiang, W. Cui, J. Q. You, and F. Nori, Phys. Rev. A **88**, 012329 (2013).